



# Multi-physics models for design basis accident analysis of sodium fast reactors. Part I: Validation of three-dimensional TRACE thermal-hydraulics model using Phenix end-of-life experiments

Sara Silva Pinto Wahnou<sup>a,b,\*</sup>, L. Ammirabile<sup>a</sup>, J.L. Kloosterman<sup>b</sup>, D. Lathouwers<sup>b</sup>

<sup>a</sup> European Commission, Joint Research Center, Nuclear Safety and Security, Nuclear Reactor Safety and Emergency Preparedness, Westerduinweg, PO Box-2, 1755 Petten, The Netherlands

<sup>b</sup> Delft University of Technology, Department of Radiation Science and Technology, Mekelweg 15, 2629JB Delft, The Netherlands

## ARTICLE INFO

### Keywords:

Sodium fast reactor  
TRACE  
Phenix end-of-life natural circulation test  
Model validation  
Three-dimensional thermal  
Hydraulics model

## ABSTRACT

The demonstrated technological feasibility of Sodium-cooled Fast Reactors (SFRs) makes them stand out among the other reactor concepts proposed by Generation IV International Forum (GIF) for short-term deployment. The availability of reliable computational tools in support of safety analyses and plant simulations under complex transient scenarios is essential to assure SFR's compliance with the highest safety goals.

Answering this need, a multi-physics three-dimensional core and system model is being developed to enable a more detailed representation of the physics of the plant and to anticipate more accurately plant behaviour, even under wider three-dimensional scenarios, such as asymmetric transients. The coupling will be performed using the U.S.NRC system codes TRACE-PARCS, modified to simulate more accurately when using sodium as coolant.

The publicly available end-of-life tests conducted in the French SFR Phenix were chosen as baseline to perform a first validation of the computational model. The development of the tool started with a three-dimensional thermal-hydraulic nodal system of Phenix using the TRACE system code.

The system simulates the Phenix end-of-life natural circulation test and the result have been compared with published experimental and benchmark results. The main physical phenomena of the 3 phases of the transient (rise in temperature in the low part of the reactor vessel, establishment of natural convection and subsequent cooling of the lower and upper part of the vessel) are predicted by the developed nodal system. More specifically, the analysis of parameters such as Intermediate Heat Exchangers (IHX), primary pumps and core temperatures, shows that the developed system is able to predict and study natural convection phenomena in Phenix-type reactors.

The three-dimensional nodal system is able to clearly illustrate the existing thermal stratification in the hot pool, which is neglected by one-dimensional systems and enables the modelling of thermal hydraulic asymmetric behaviour, as it is shown by the uneven flow distribution in Phenix's primary IHXs as they are asymmetrically located in the reactor vessel.

## 1. Introduction

As an energy source and demonstrated value of more than 50 years of commercial power production, nuclear power may play an important role in the future low-carbon energy mix. Recognizing it, several countries are carrying out R&D programs to prepare the deployment of a new generation (Generation-IV) of nuclear advanced systems, that could excel in terms of sustainability, safety and reliability, economics and proliferation resistance and physical protection.

The Generation-IV International Forum (GIF) was launched in 2001 focusing on collaborative R&D programs for selected innovative reactor systems. GIF has selected six reactor concepts for near future large scale implementation, conceived to excel in their reliability, sustainability, safe operation, economic competitiveness and proliferation resistance (Generation-IV International Forum, 2014).

The Sodium-cooled Fast Reactor (SFR) design stands out among the reactor concepts selected by GIF based on its technological feasibility demonstrated in several countries during the last decades. In order to

\* Corresponding author at: European Commission, Joint Research Center, Nuclear Safety and Security, Nuclear Reactor Safety and Emergency Preparedness, Westerduinweg, PO Box-2, 1755 Petten, The Netherlands.

E-mail addresses: [S.SilvaPintoWahnou-1@tudelft.nl](mailto:S.SilvaPintoWahnou-1@tudelft.nl) (S. Silva Pinto Wahnou), [L.Ammirabile@ec.europa.eu](mailto:L.Ammirabile@ec.europa.eu) (L. Ammirabile), [j.l.kloosterman@tudelft.nl](mailto:j.l.kloosterman@tudelft.nl) (J.L. Kloosterman), [D.Lathouwers@tudelft.nl](mailto:D.Lathouwers@tudelft.nl) (D. Lathouwers).

<https://doi.org/10.1016/j.nucengdes.2018.02.038>

Received 26 July 2017; Received in revised form 18 February 2018; Accepted 24 February 2018

Available online 20 March 2018

0029-5493/ © 2018 The Author(s). Published by Elsevier B.V. This is an open access article under the CC BY license (<http://creativecommons.org/licenses/by/4.0/>).

assess the compliance of the SFR design with Generation IV safety goals, it is necessary to identify and analyze plant behavior against potential accident scenarios. In this respect, the development and validation of computational tools able to perform reliable plant behavior simulations is essential to the safety case.

To enable a more detailed representation of the physics of the plant and to simulate more accurately plant behavior, even under 3-dimensional scenarios such as asymmetric transients, a doctoral work is aiming at the development and validation of a multi-physics three-dimensional core and system model of a SFR, combined features still not yet validated by current computational tools. This paper describes the first step of the tool development, specifically the development of a three-dimensional thermal-hydraulics nodal system of the French SFR Phenix and its validation against Phenix end-of-life (EOL) natural circulation test. The computational tool used in the present study is an adaptation of the U.S. Nuclear Regulatory Commission (NRC) thermal-hydraulics system code TRACE to simulate more accurately when using sodium as coolant. The second step of the development features the coupling of the U.S. NRC system codes TRACE-PARCS, matter that will be described in a future paper.

### 1.1. Sodium fast reactors

As the name describes, the SFR operates with a fast neutron spectrum, which not only allows energy production but also breeding, as the conversion rate of fertile material into fissile ( $^{238}\text{U}$  into  $^{239}\text{Pu}$ ) can be greater than the fissile consumption rate from the fission chain reaction. Additionally, it also features transmutation capabilities, contributing positively to nuclear waste management. Typically, a SFR operates at a near to atmospheric pressure in the primary system and at temperature of 550 °C, contrasting with the 15 MPa and 350 °C of the PWR operation conditions. This results in producing a higher temperature steam, increasing the energy conversion efficiency.

Throughout the past 50 years, the development of Liquid Metal Fast Reactors (LMFRs) enabled to acquire more than 300 reactor-years of operating experience. The first SFR, the EBR-I, was built in the U.S. and reached criticality in 1951 (International Atomic Energy Agency, 2006). Since then, several fast programs were launched in Asia and Europe (International Atomic Energy Agency, 2006). In Europe, France is the European country that invested the most in SFR development up to now. Its history with SFRs started with the experimental reactor Rapsodie, which started operation in 1967 till 1983 (International Atomic Energy Agency, 2012). This was continued by Phenix prototype, reaching criticality in 1973 and shutdown in 2009 (International Atomic Energy Agency, 2013). Its 35 years of successful operation demonstrated the viability of sodium-cooled fast breeder reactors. In July 2009, Phenix was disconnected from the grid and was prepared for a set of final tests. These tests were projected and carried out as a unique opportunity to learn more about the prototype and contribute to the future development of SFRs. For this reason, Phenix prototype reactor was chosen to be the reference reactor for the model development in this study, validated against some of the Phenix end-of-life tests. The success of Rapsodie and Phenix led to the design and construction of the first large industrial fast breeder worldwide, the Superphenix, having reached criticality in 1985 (International Atomic Energy Agency, 2012). Technical incidents and public opposition dictated the fate of Superphenix that was shut down in 1997, 20 years before the end of the plant's designed lifetime. Nonetheless, Superphenix was still able to demonstrate that large scale fast reactors are possible to operate neutronics wise, as the large thermal inertia limits greatly the reactivity feedback effects. In addition, the European Fast Reactor (EFR) project was launched in 1988 by the European Fast Reactor Utilities Group (EFRUG) (Lefèvre et al., 1996), having the French electric utility company EDF as leader. The EFR design aimed to gather the combined experience of France, Germany and the UK for liquid metal reactor technology based on pool-type reactors. The developed design was

based on established technology and with realistic cost estimates (Lillington, 2004). Although its construction is not foreseen in the near future, the project constituted an important step towards the road of the commercial utilization of fast reactors. Presently, France is working on the Advanced Sodium Technological Reactor for Industrial Demonstration (ASTRID) Project (International Atomic Energy Agency, 2012). The project aims to develop a SFR industrial prototype (ASTRID) expected to serve as a precursor of a first-of-its-kind commercial reactor that can meet GIF's criteria.

Joint European efforts have also been made towards SFR R&D. In 2009 10 different countries engaged in a collaborative project within EURATOM's 7th Framework program for nuclear and research training for the development of a Gen-IV European Sodium-cooled Fast Reactor (ESFR) (CEA, 2003–2011). The project targeted the deployment of ESFR technology by mid-century and finished successfully in 2013. A continuation of ESFR Project was launched in 2017 with the collaborative Project ESFR-SMART (Mikityuk, 26–29 June 2017).

#### 1.1.1. Calculation tools for sodium fast reactors

Many computational tools dedicated to SFR analysis have been developed throughout the years of SFR R&D. Code developments have been focusing on different type of accident analysis, simulating different relevant phenomena. Among the available computational tools, it is possible to distinguish purely thermal-hydraulic codes, purely neutronic codes and coupled thermal-hydraulic/neutronics codes. Additionally, it is possible to distinguish codes of different types, e.g. deterministic versus statistic, the scale of each computational tool, steady state versus transient, etc., and if they are applicable to the full core or to the full reactor. The analysis of Generation-IV SFRs would benefit by the use of multi-physics models, like the coupling between thermal-hydraulic and neutronics computation tools.

The most important experimental and theoretical findings related to sodium have been integrated to state-of-the-art codes, of which SAS4A/SASSYS-1 (Cahalan et al., 2000) and SIMMER-III/IV (Tobita et al., 2006) appear as reference tools. SAS4A and SASSYS-1 computer codes were first developed at ANL for the transient analysis of LMFRs. SAS4A analysis has the objective to quantify severe accident consequences as measured by the generation of energy sufficient to challenge reactor vessel integrity; whereas SASSYS-1 analysis is to quantify accident consequences as measured by the transient behavior of system performance parameters, such as fuel and cladding temperatures, reactivity and cladding strain. In spatial terms, each SAS4A/SASSYS-1 channel models a fuel pin and its associated coolant. These two codes have been additionally coupled to nodal spatial kinetics computer codes (VARIANT-K and DIF3D-K) for accurate analysis of coupled spatial neutron kinetics and thermal hydraulic effects. For Core Disruptive Accidents (CDA), SIMMER has been developed continuously since its first release (Bohl and Luck, 1990). The current code version allows an evaluation of the transition phase of a CDA, through the simulation of the entire core and the modelling of key thermodynamic and neutronics phenomena occurring during the accident progression.

The FAST (Fast-spectrum Advanced Systems for power production and resource management) code system is currently being developed at PSI for static and transient analysis of Design Basis Accidents (DBA) of the main Generation-IV fast-neutron spectrum reactor concepts: sodium, gas and lead-cooled fast reactors. The main goal is to allow an analysis of advanced fast spectrum systems including different coolants and fuel types. The reactor modelling includes an integral representation of the core neutronics, thermal-hydraulics and fuel behavior, and the reactor primary and secondary systems. The code system has been assembled from well-established existing codes, extended to the simulation of fast reactor features when necessary, namely: ERANOS, for static neutronics, PARCS, for reactor kinetics, TRACE, for system thermal-hydraulics, and FRED, for thermal mechanics.

The procedure followed in this study has been based on the adaptation of computational tools verified, validated and extensively used in





fluid, conduction and kinetics equations are averaged. TRACE database includes physical properties for several coolants, including liquid sodium. However, some physical correlations/models had to be updated and/or added in order to perform more accurate simulations.

#### Heat transfer models

For liquid metals heat transfer in pipes, TRACE yields for the calculation of the Nusselt number the correlation (U.S.NRC, 2012):

$$Nu = 4.8 + 0.025 \cdot Pe^{0.25}, \quad \text{where } Nu \text{ and } Pe \text{ are the Nusselt and Peclet numbers} \quad (1)$$

The correlation (1) was considered valid for liquid metals' pipe flow. However, following literature recommendations (Mikityuk, 2009), it was implemented a more appropriate correlation for liquid metals in bundle flow – the Ushakov correlation:

$$Nu = 7.55x - \frac{20}{x^{13}} + \frac{0.041}{x^2} \cdot Pe^{0.56+0.13x}, \quad (2)$$

where,

$$x = \frac{P}{D} = 1.1-1.95, \\ Pe = \text{Peclet number} = \text{range}(30-5000).$$

#### Liquid sodium internal energy calculation

From previous applications of TRACE in liquid metal cooled fast reactors modelling (Lazaro et al., 2013) it was noticed an over-estimation of the coolant's temperature. After analysis, it was concluded that this was due to a crude calculation of the fluid's (sodium) internal energy that lead to an underestimation of its internal energy.

Originally, TRACE calculates the liquid sodium internal energy simply as the integral of a reference specific heat:

$$U_{INa} = c_{pR} \cdot (T_l - T_R) + U_{SR} \quad (\text{U. S. NRC, 2012}), \quad (3)$$

where,

$$U_{INa} \text{ is the liquid sodium internal energy,} \\ c_{pR} = 1150.9452 \text{ J/(kg} \cdot \text{K)} \text{ is the reference specific heat,} \\ T_l \text{ is the liquid temperature,} \\ T_R = 371 \text{ K is the reference temperature,} \\ U_{SR} \text{ is the saturation liquid energy at reference temperature.}$$

The correlation (3) was improved by calculating the liquid sodium internal energy in means of TRACE's sodium specific heat correlation analytical integral:

$$U'_{INa} = \left[ \int c_{pINa} \right]_{T_l} - \left[ \int c_{pINa} \right]_{T_R} + U_{SR}, \quad (4)$$

where,

$$U_{INa} \text{ is the liquid sodium internal energy,} \\ T_l \text{ is the liquid temperature,} \\ T_R = 371 \text{ K is the reference temperature,} \\ U_{SR} \text{ is the saturation liquid energy at reference temperature,} \\ c_{pINa} \text{ is TRACE's liquid sodium specific heat correlation:}$$

$$c_{pINa} = 1646.97 - 0.831587T_l + 4.31182 \times 10^{-4}T_l^2 \quad (\text{U. S. NRC, 2012}). \quad (5)$$

#### Pressure correlation

From literature review and previous benchmark calculations (Lazaro et al., 2013), it was concluded that the pressure drop model along fuel elements (wire-wrapped) should be updated.

Given how TRACE calculates pressure losses along fuel elements (U.S.NRC, 2012), it was understood that the fault was due to an inappropriate model of the friction factor, used for the calculation frictional pressure loss due to shear stress at the wall. The friction factor  $f_j$  is originally calculated in TRACE using the Churchill correlation (U.S.NRC, 2012):

$$f_{\text{Churchill}} = 2 \left( \left( \frac{8}{Re} \right)^{12} + \frac{1}{(A+B)^{1.5}} \right)^{\frac{1}{12}}; \\ A = \left( 2.457 \cdot \ln \left( \frac{1}{\left( \frac{7}{Re} \right)^{0.9} + 0.27 \cdot \frac{\epsilon}{D_h}} \right) \right)^{16}; \quad B = \left( \frac{37530}{Re} \right)^{16} \quad (6)$$

where,

$$D_h \text{ is the hydraulic diameter [m],} \\ \epsilon \text{ is the surface roughness [m],} \\ Re \geq 5000 \text{ is the Reynolds number.}$$

According to (Bubelis and Schikorr, 2008), it was verified through experimental data that the friction-factor for wire-wrapped fuel assemblies having sodium as coolant is better modelled by Rehme correlation, that was then implemented in TRACE system code:

$$f_{\text{Rehme}} = \left( \frac{64}{Re} F^{0.5} + \frac{0.0816}{Re^{0.133}} F^{0.9335} \right) \cdot \left( \frac{N_r \pi (D_r + D_w)}{S_t} \right), \\ F = \left( \frac{P_t}{D_r} \right)^{0.5} + \left[ \frac{7.6(D_r + D_w)}{H} \left( \frac{P_t}{D_r} \right)^2 \right]^{2.16}, \quad (7)$$

where,

$$H \text{ Wire lead length (pitch) [m]} \\ S_t \text{ Total wetted perimeter [m]} \\ N_r \text{ Number of fuel pins} \\ D_r \text{ Rod diameter [m]} \\ D_w \text{ Wire (spacer) diameter [m]} \\ P_t = D_r + 1.0444 \cdot D_w \text{ Rod pitch wire-wrap configuration [m].}$$

### 2.1. Phenix thermal-hydraulic nodal systems

Following Phenix benchmark specifications (International Atomic Energy Agency, 2013), the Phenix thermal-hydraulics modelling started with a one-dimensional nodal system that, after its validation, was expanded to a three-dimensional representation. Below both one- and three-dimensional thermal-hydraulics nodal systems are described. Transient calculation results of both systems will be later compared to each other, to some of the CRP benchmark results and to the experiment.

#### 2.1.1. One-dimensional TRACE/thermal-hydraulics nodal system

Fig. 2 shows schematically the developed one-dimensional thermal-hydraulics Phenix nodal system. The system includes the primary system and a simplified secondary. Both primary and secondary loops were modelled with single components – 1 primary pump, 1 IHX and 1 secondary – with the corresponding weights to account for the actual 6

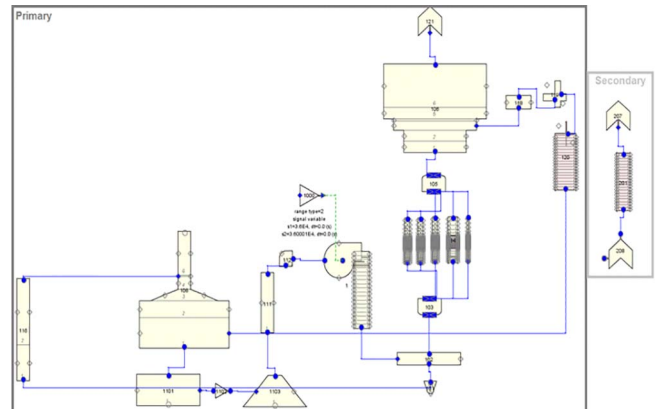


Fig. 2. Phenix one-dimensional thermal-hydraulic nodal system (TRACE).

**Table 2**  
Onedimensional model core channels description.

Channel	Flow Area (m <sup>2</sup> )	Hydraulic Diameter (m)	Power Fraction	Length (m)	
				Total	Active
1 Fuel inner core	0.269	$4.09 \times 10^{-3}$	0.517	3.517	0.85
2 Fuel outer core	0.280		0.409		
3 Fertile zone	0.319	$4.97 \times 10^{-3}$	0.069		
4 Reflector zone	0.926	$1.399 \times 10^{-1}$	0.003		
5 Control rods	0.031		0.002		

IHX, 3 primary pumps and 3 secondary loops.

The Phenix core is modelled by a set of five parallel PIPE components (one-dimensional channels), each one attached to an individual heat structure component, all powered by a single power component. Table 2 describes the 5 core channels. The core division was chosen by having one channel for each core zone to simplify the model as the interest lies in the whole system behavior. The flow distribution among the core zones (International Atomic Energy Agency, 2013) was achieved by the use of K loss coefficients at the bottom of each channel to simulate the gagging at the front edge of each channel (International Atomic Energy Agency, 2013). The imposed power is distributed among the different channels as shown in Table 2.

The core components are connected to the hot (upper) and cold (lower) plena. The hot plenum is divided into 3 regions: one to model the volume of the pool over the core and other two that model the structures that convey the coolant from the core to the primary side of the IHX where the heat is transferred to the secondary circuit. From the primary side of the IHX, the coolant reaches the cold plenum, modelled by 8 channels, conveying it to the core inlet. The coolant flow path connects the end of the cold plenum to its top. The secondary systems are represented by a single channel, with equivalent dimensions to the 3 existing secondary loops. The boundary conditions for secondary mass flow and pressure are imposed. The primary pump was modelled by a TRACE pump component, with equivalent weight to the 3 Phenix primary pumps following primary pump specifications (using the homologous representation) (U.S.NRC, 2012).

### 2.1.2. Three-dimensional TRACE/thermal-hydraulics nodal system

The methodology followed to build the three-dimensional thermal-hydraulics nodal system was to expand the developed one-dimensional system into a three-dimensional one. To achieve this, the TRACE component VESSEL was used. The VESSEL component is three-dimensional and can be discretized axially, radially and azimuthally. Components like the core, diagrid, hot and cold plena were converted into VESSEL nodes with appropriate volumes and flow areas. The other components – primary pumps, primary IHXs and simplified secondary – were left as one-dimensional components, connected to the correspondent VESSEL cells. Each Phenix primary pump was modelled individually following the specifications and using TRACE's PUMP component. Additionally, three primary IHXs were modelled, each with a factor of 2, and, consequently, three simple secondary circuits. It is important to highlight that, according to Phenix specifications (International Atomic Energy Agency, 2013), only two IHX pairs are in function, thus, only two of the modelled IHX will be connected to the VESSEL.

All one-dimensional system characteristics mentioned in the section before were adapted to be consistent with the three-dimensional configuration. The three-dimensional TRACE nodal system is shown in Fig. 3. The three primary IHXs and secondary systems are highlighted in red. The three primary pumps are highlighted in green and the VESSEL component in blue. The VESSEL was divided in 29 axial levels, 7

(radial) rings and 3 azimuths. Each modelled primary IHX and primary pump was connected to one VESSEL azimuth. VESSEL axial discretization is shown and described in Fig. 4. The core is modelled between VESSEL's axial levels 3 and 23 and rings 1 to 5, across its three azimuths. In this model, each third of ring across the core axial levels has associated a heat structure component that models all pins individually contained in that respective core zone, with their specific structure (materials and geometry), similarly to what was done in the one-dimensional nodal system.

## 3. Model validation

To test the developed model and computational tool capabilities (under development), Phenix end-of-life natural circulation test was simulated. Below, calculation results are compared to the experiments and to some of the CRP benchmark results (International Atomic Energy Agency, 2013).

### 3.1. Initial and boundary conditions

To simulate the natural circulation test with the developed models, the thermal power, secondary inlet temperature and mass flow rate were given as input. These parameters were set according to the measured test results (International Atomic Energy Agency, 2013). Figs. 5–7 show their evolution from the beginning till the end of the test.

### 3.2. Results comparison

#### 3.2.1. Steady state results

TRACE three-dimensional nodal system steady state results of the initial state of the natural circulation test are presented and compared to Phenix nominal conditions in Table 3. The margins acceptable for the parameters are (International Atomic Energy Agency, 2013) (D'Auria et al., 1999):

- Calculated temperatures  $\pm 5$  degrees from the nominal value;
- Mass flows with deviations smaller than 2% of the nominal value;
- Calculated core pressure drop with maximum 10% deviation of nominal value.

The calculated steady state temperatures and mass flows shown in Table 3 are within the accuracy limits, demonstrating the reliability of the system predicting these parameters. However, the predicted core pressure drop falls out of the acceptable error margin. In fact, there is no information of where the core pressure should be taken from exactly, thus it is possible that the calculated value shown in Table 3 does not reflect the nominal core pressure drop given in the benchmark specifications (International Atomic Energy Agency, 2013). The core pressure drop drives the system, which needs to compensate the pressure to achieve the correct system mass flow due to the use of K loss coefficients for core flow distribution that increase the core pressure drop.

#### Natural circulation simulations

The transient's main physical phenomena are described in this section. Furthermore, simulation results of the developed models of different parameters relevant to reactor behavior are analyzed and compared to experimental results and other institutions' calculations of the CRP benchmark.

#### Transient's main physical phenomena

During the first phase of the test, the dry-out of the SGs in function causes a loss of heat sink, leading to heating of the lower part of the reactor vessel. Consequently, the increase of core inlet temperature leads to a drastic decrease of core power, result of the neutronics feedback. Since the core power was given as input, the latter physical phenomena cannot be confirmed by the developed TRACE models. However, it is possible to confirm the trend of rise in temperature in the lower part of the reactor vessel, as seen in Fig. 8. There, the extracted

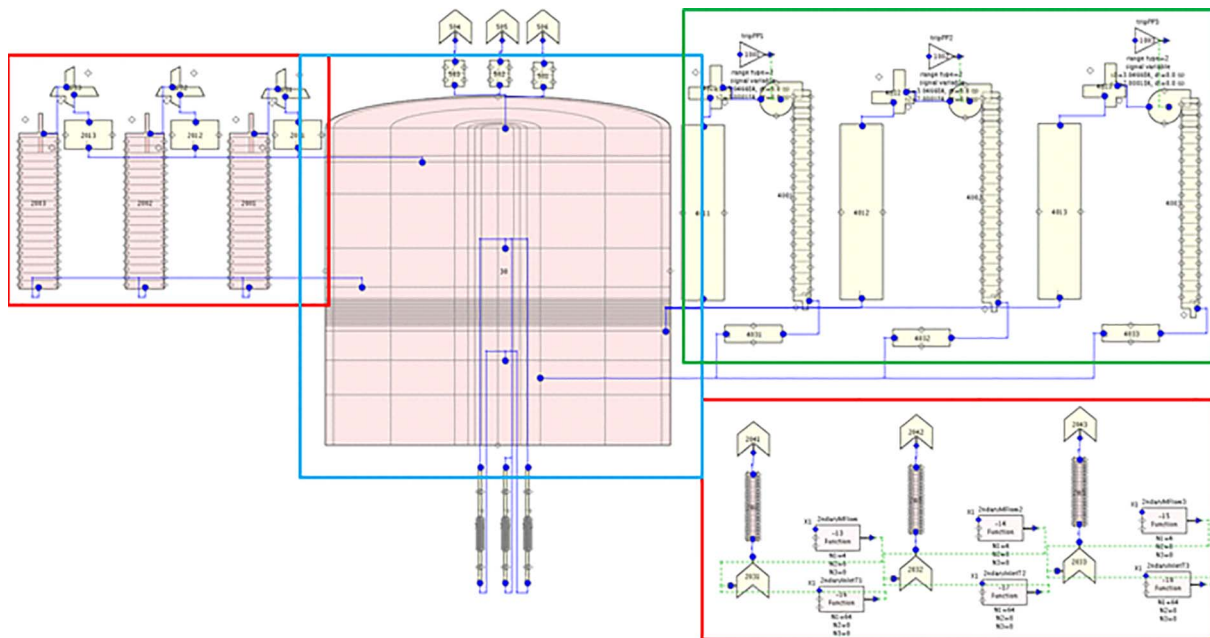


**Fig. 3.** Phenix three-dimensional TRACE nodal system.

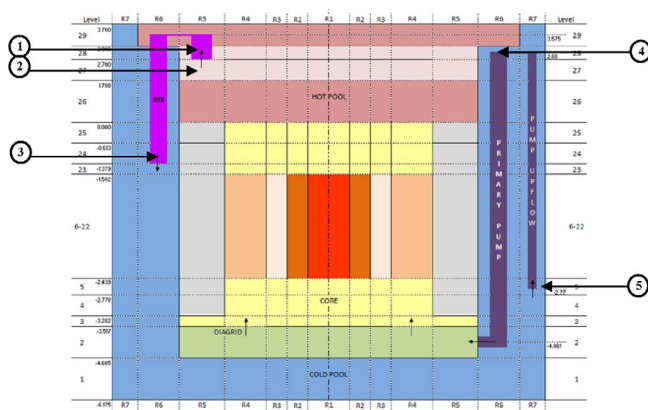


**Fig. 4.** TRACE VESSEL component axial discretization.

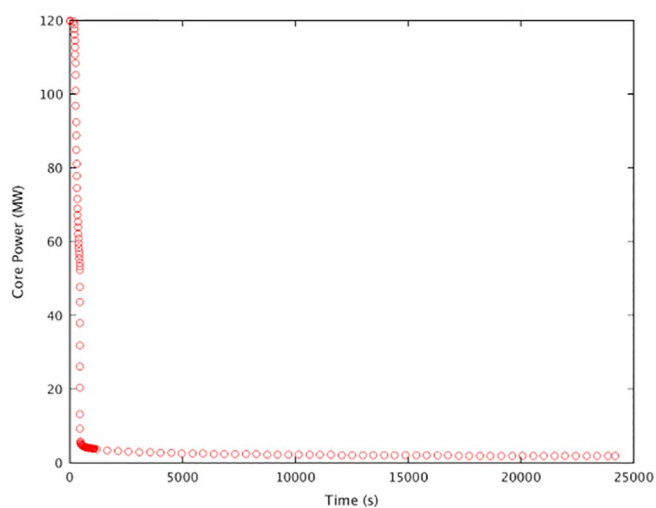


**Fig. 5.** Thermal power input throughout the natural circulation test (International Atomic Energy Agency, 2013).

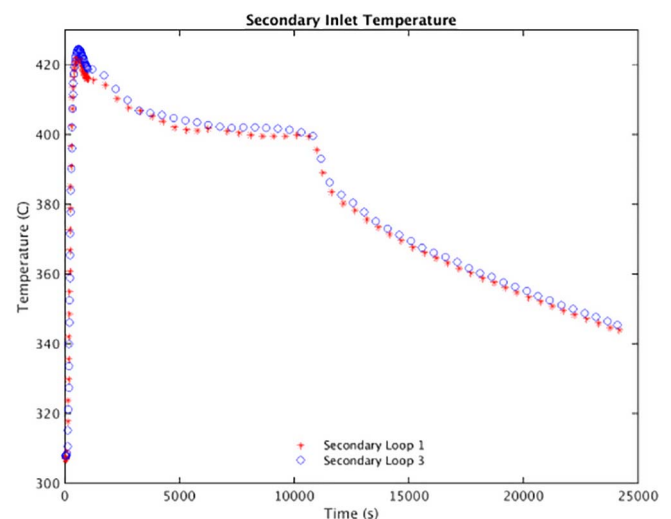


**Fig. 6.** Secondary inlet temperature evolution of both secondary loops in service during the natural circulation test (International Atomic Energy Agency, 2013).

experimental results during the first phase of the transient are compared to the results of TRACE three-dimensional nodal system, extracted from location 5 marked in Fig. 4. Nevertheless, it is expected a discrepancy in results as it is not known the exact location where the temperatures are measured.

The establishment of natural convection occurs in the test's second phase. Two thermal shocks take place in the beginning of this phase. The first, classified as cold shock, due to the manual activated scram is closely followed by the second, a hot shock, due to the trip of the pumps. This behavior can be observed in Fig. 11, where TRACE calculations are compared to the experiments. In the long term, it is reached an equilibrium state, where the whole reactor vessel gets progressively homogeneous, a behavior which can be observed also in Fig. 9, by the plateau region up to 10 000 s of the transient.

The third (last) phase of the natural circulation test is initiated by the opening of the SGs' casings that leads to a recovery of an efficient heat sink. As consequence, the lower part of the vessel starts to cool followed by the cooling of the upper part of the vessel, observed [Figs. 9](#)

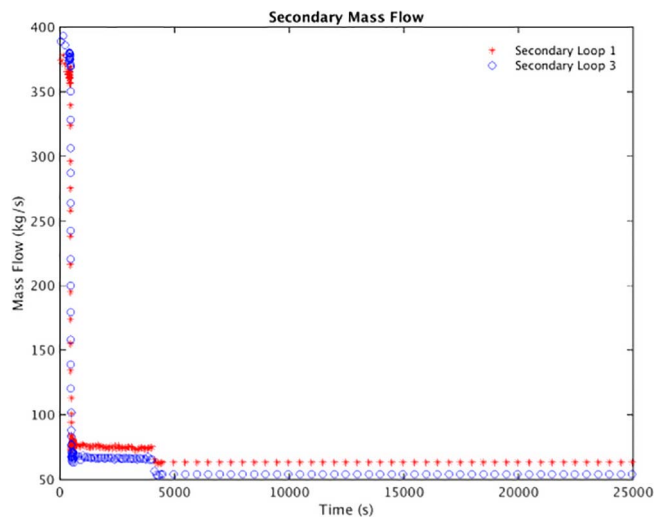


Fig. 7. Secondary mass flow evolution of both secondary loops in service during the natural circulation test (International Atomic Energy Agency, 2013).

and 10, from the 10 000 s of the start of the transient onwards.

#### Core pressure drop and mass flow

Fig. 11 shows the core pressure drop and mass flow evolution, on the left and right, respectively, of TRACE simulations (both one- and three-dimensional nodal systems) in comparison to other institutions' results throughout the natural circulation test. It should be noted that there is no experimental data available of neither these parameters so comparisons are only possible among different codes' simulations.

The plot on the left of Fig. 11 features the core pressure drop evolution during the transient. The TRACE results correspond to pressure differences between different core regions and core heights, showing a big variation in results depending where the pressure is extracted. This demonstrates the ambiguity associated to this parameter since it is unknown what is understood by core pressure drop specifically. This associated to the fact that all other institutions' results come from 1-dimensional systems, it is hard to compare quantitatively the results in detail. As explained in Section 2, TRACE pressure friction factor correlation was updated to the Rehme correlation for sodium flow in bundle geometry proven by literature (Bubelis and Schikorr, 2008) to be the most appropriate for this case. However, it is not known which correlations were used by other institutions' codes. Qualitatively, in comparison to other institutions' calculations, TRACE calculations exhibit the same behavior - steep reduction of core pressure drop after the trip of the primary pumps, followed by a stable core pressure drop. For the developed three-dimensional thermal-hydraulics nodal system, in

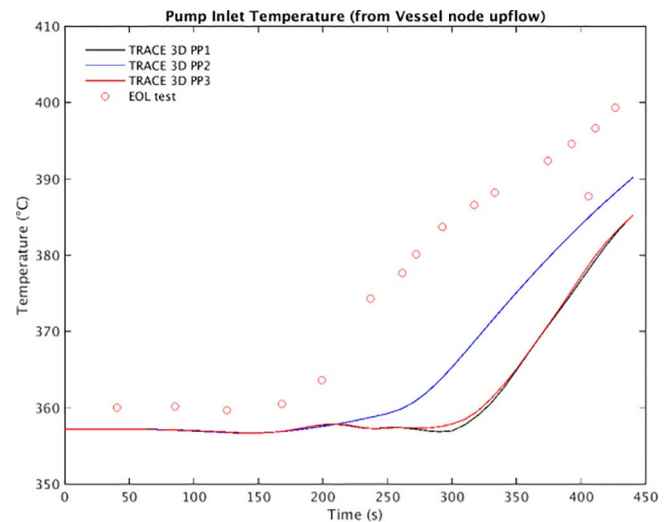


Fig. 8. Evolution of the pump inlet temperature during the 1st phase of the natural circulation test. TRACE results extracted from nodal system's location 5 as seen in Fig. 4. Experimental results extracted from (International Atomic Energy Agency, 2013).

natural circulation regime the pressure drop of the inner fuel at active core height stabilizes at  $\sim 0.10$  bar, while at full core height at  $\sim 0.27$  bar.

The core mass flow evolution during the transient is featured on the plot of the right of Fig. 11. The mass flow of the TRACE three-dimensional nodal system is set correctly on the natural circulation initial state, demonstrating a correct set up of the primary pumps and flow distribution between core and cooling flow path. With the trip of the primary pumps, the mass flow evolution of TRACE calculations follows the other institution's calculations and the three-dimensional system predicts a core mass flow in natural circulation of 41 kg/s,  $\sim 3\%$  of core initial mass flow. This is comparable to the other benchmark results that lie within 2–4% of their initial core mass flow. TRACE one-dimensional system results show a bigger discrepancy than the three-dimensional nodal system compared to the other institutions' results – the imposition of higher K loss coefficients to establish the correct flow distribution in the core that cause the rise of core pressure drop, and its close relation to the core mass flow, is more visible in the one-dimensional system.

#### Core outlet temperature

The core outlet temperature throughout the transient is shown in Fig. 9. The experimental results are based on monitored fuel assemblies, therefore the results do not represent the behavior of the whole core.

On the left of Fig. 9, the plot shows the TRACE three-dimensional

Table 3

Steady-state parameters of Phenix initial state of natural circulation test and developed three-dimensional nodal system.

Channel	Nominal		Model		Dev (%)
Power (MW(th))	120		120.00		–
Pressure drop core (bar)	0.839		0.99 <sup>1</sup>		18.00
Temperature (°C)	Core inlet	358	354.64		–0.94
	Core outlet	432	430.81		–0.28
	IHX primary inlet	432	430.81		–0.28
	IHX primary outlet	360	356.85		–0.88
	Secondary inlet	308	308.00		–
	Secondary outlet	432	429.68		–0.54
	Primary	1426.67	1417.30		–0.66
	Secondary	760	760.00		–
	Core	1284	1264.45		–1.52
	Mass Flow Fraction		Mass Flow Fraction		Deviation in Mass Flow Fraction
Fissile	1055	0.74	1021.99	0.72	0.02
Fertile	149	0.10	158.68	0.11	0.01

<sup>1</sup> Pressure drop of the fuel region of the active core.



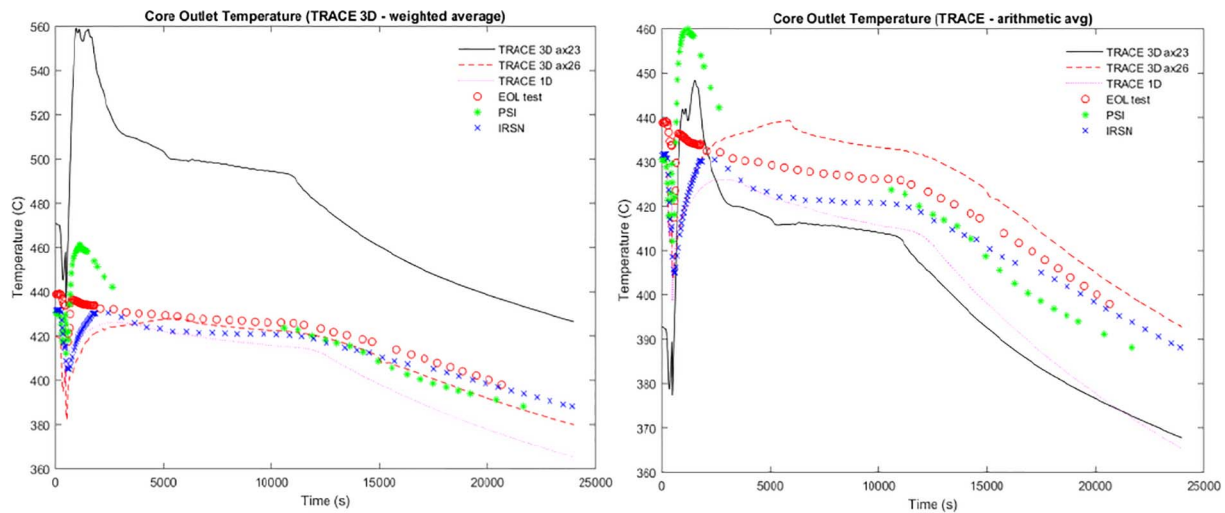


Fig. 9. Core outlet temperature evolution throughout the natural circulation transient. On the left, the TRACE three-dimensional results are weightily averaged over the different core regions taking into consideration their mass flows. On the right, the average is done arithmetically. Other institutions' results taken from (International Atomic Energy Agency, 2013).

nodal system core outlet temperature mass weighted average in each core region in different two different axial levels, the results of TRACE one-dimensional nodal system, the test's experimental results and other institutions' simulation results. The plotted temperature for core axial level 23 is located just over the active core, while axial level 26 is located over the full core height. The discrepancy between the two sets of results show how important is the coolant mixing effect and how challenging it is to compare results from a three-dimensional system to a one-dimensional one.

According to literature (International Atomic Energy Agency, 2013), the experimental Phenix core outlet temperature is obtained by a simple arithmetic average over the core, not taking into account the mass flow in each region. The plot on the right hand side of Fig. 9 features then the TRACE three-dimensional nodal system core outlet temperature arithmetic average over the core of also axial levels 23 and 26. In this plot, the temperatures are of comparable range of experimental results and results of the one-dimensional codes. In this case, the mixing effects are also visible, as the results of axial level 23 and axial level 26 are reasonably different. It is understandable why the weighted average leads to higher temperatures: the regions that contain most of the mass flow are the ones with higher outlet temperature (inner and outer fuel).

Regarding the three-dimensional nodal system results behavior,

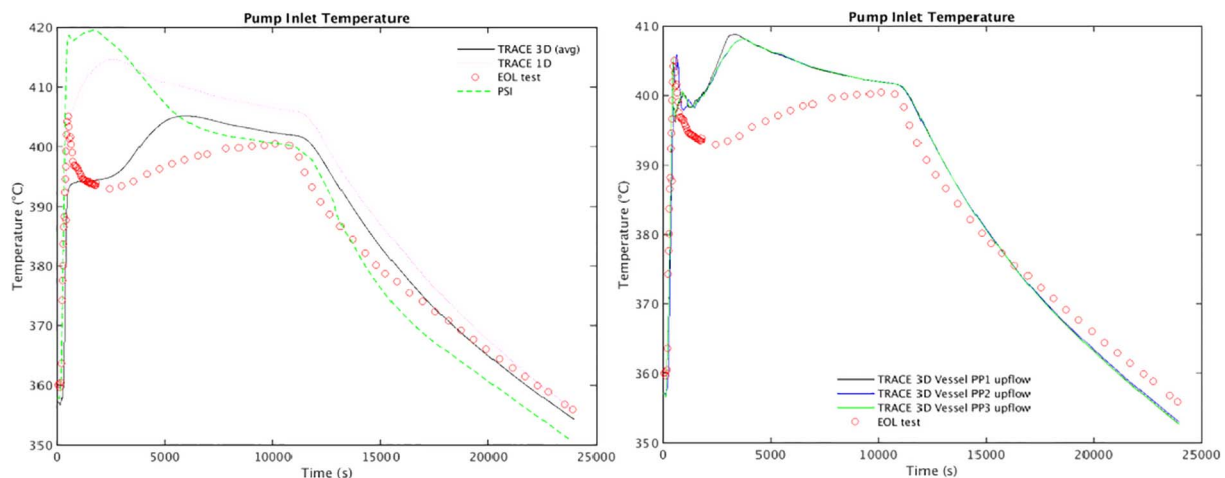


Fig. 10. Primary pumps inlet temperature evolution during the natural circulation test. On the left, TRACE's three dimensional nodal system results is the average temperature at the three primary pumps inlet (location 4 marked in Fig. 4), while on the right, TRACE's three-dimensional nodal system temperatures are extracted on the vessel nodes from where the coolant is conveyed to the primary pumps (location 5 marked in Fig. 4). Other institutions' results taken from (International Atomic Energy Agency, 2013).

Fig. 12 features on the left the first 600 s of the transient and on the right, the first 10 000 s. It is possible to observe that in the first 350 s the cold shock is predicted although the temperatures are overall underestimated. Additionally, the scram is well reproduced (prediction of sharp drop in temperature and two thermal shocks). From the scram till ~300 s after the start of the transient, there is an increase of temperature caused by the reduction of the flow rate. The temperature discrepancies between calculation and experimental results may be due to the fact that measurements only monitor certain fuel assemblies and there is no information about their location.

#### Primary IHX inlet temperature

The evolution of primary IHXs inlet temperature throughout natural circulation transient is shown in Fig. 13.

On the left plot of Fig. 13, experimental results, TRACE three-dimensional nodal system calculation's results and other institution's calculations results are showed against the calculated temperatures at the inlet of the two operating IHXs by TRACE's three-dimensional nodal system (location 1 marked in Fig. 4). The contrasting inlet temperatures of the IHXs are due to an asymmetric mass flow distribution among them due to the inherent asymmetric geometry of the system. Taking the average inlet temperature of the two primary IHXs, it is possible to verify that it follows the core outlet temperature, shown in Fig. 9. It is important to notice that according to the calculations, the cold shock



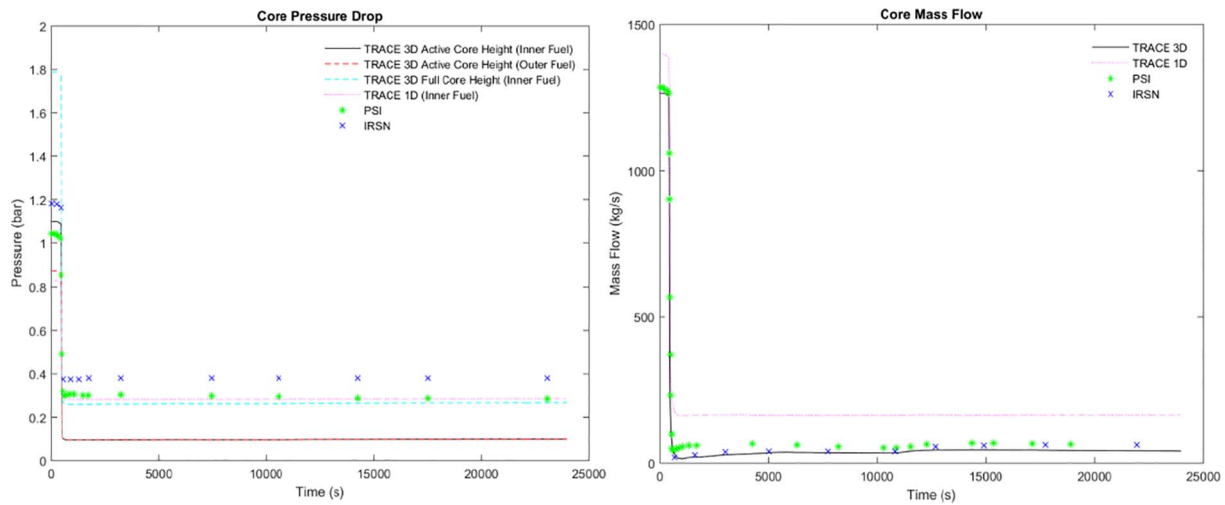


Fig. 11. Core pressure drop, on the left, and core mass flow, on the right, evolutions during the natural circulation test simulation. Other institutions' results taken from (International Atomic Energy Agency, 2013).

due to decrease of power at the beginning of the transient is propagated from the core outlet to the IHXs inlet, a behavior that is not confirmed by the experimental results. This may be explained by the fact that the thermocouple measuring the IHX inlet temperature is located in the upper part of the IHX window where temperature and mass flow rate heterogeneities appear. As a consequence, the measurements are not necessarily representative of the average temperature at the IHX inlet.

To demonstrate the coolant mixing effects in the hot pool the averaged calculated temperature on the vessel nodes (of TRACE's three-dimensional nodal system) from where the coolant is conveyed to the primary IHXs (location 2 marked in Fig. 4) is shown on the right-hand side of Fig. 13. It is possible to see how different the temperature evolution is in the first 10 000 s of the transient, when compared to the average temperature calculation at the primary IHXs inlets.

#### Primary IHX outlet temperature

Fig. 14 shows the averaged calculated temperature at the outlet of the primary IHXs of TRACE's three-dimensional nodal system (location 3 marked in Fig. 4) compared to other calculations and experimental results. The evolution of this parameter, whose trend is confirmed by TRACE's three-dimensional system results, follows closely the secondary inlet temperature given as boundary condition (Fig. 6). However, the exact location of the measurement is unknown, which

challenges where the calculations' temperatures should be extracted. This is reflected in the first 5000 s of the transient, where TRACE's three-dimensional system results are 10 degrees lower than the measurements. This discrepancy may be due to the wrong temperature extraction location, as there is significant thermal stratification at the primary IHXs outlet window.

Finally the decrease in temperature just in the beginning of the transient observed in the experimental results is not predicted by any simulation. This temperature decrease might be caused by cooling conducted from the cold pool, which is not modelled.

#### Primary pump inlet temperature

In Fig. 10 it is shown the evolution of the primary pumps inlet temperature during the natural circulation test. In this parameter, it is also clear the importance of where the temperature is extracted due to mixing/thermal stratification effects of the cold pool. On the left of Fig. 10, the temperature of TRACE's three dimensional nodal system is the average temperature at the three primary pumps inlet (location 4 marked in Fig. 4), while on the right, TRACE's three-dimensional system temperatures are extracted on the vessel nodes from where the coolant is conveyed to the primary pumps (location 5 marked in Fig. 4).

The temperatures extracted from TRACE's three-dimensional nodal system featured on the right plot of Fig. 10 predicts the coolant

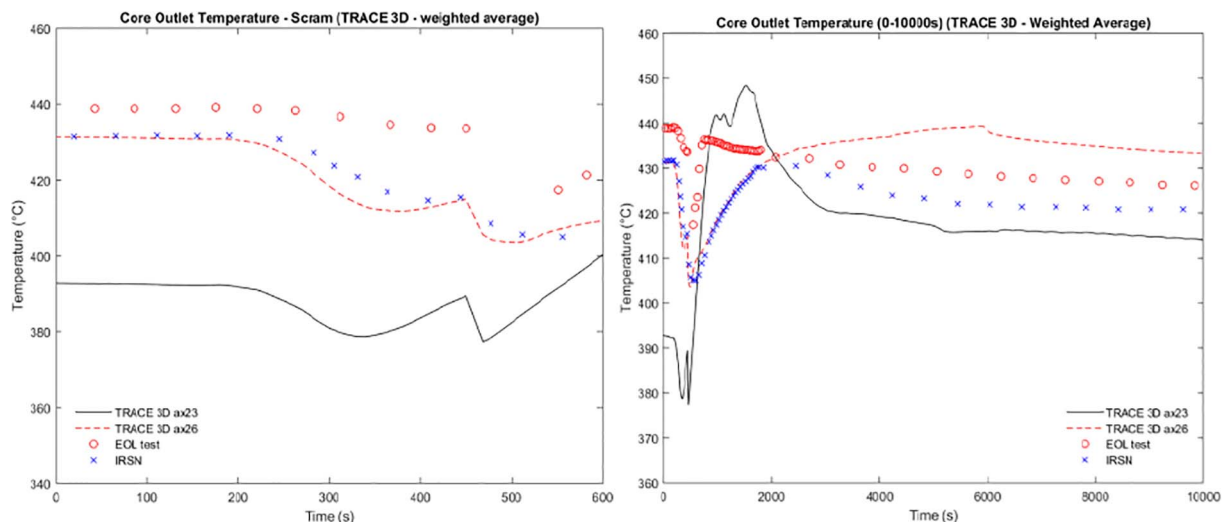


Fig. 12. Evolution of core outlet temperature during the first 600 s and 10 000 s of the transient, respectively. Other institutions' results taken from (International Atomic Energy Agency, 2013).

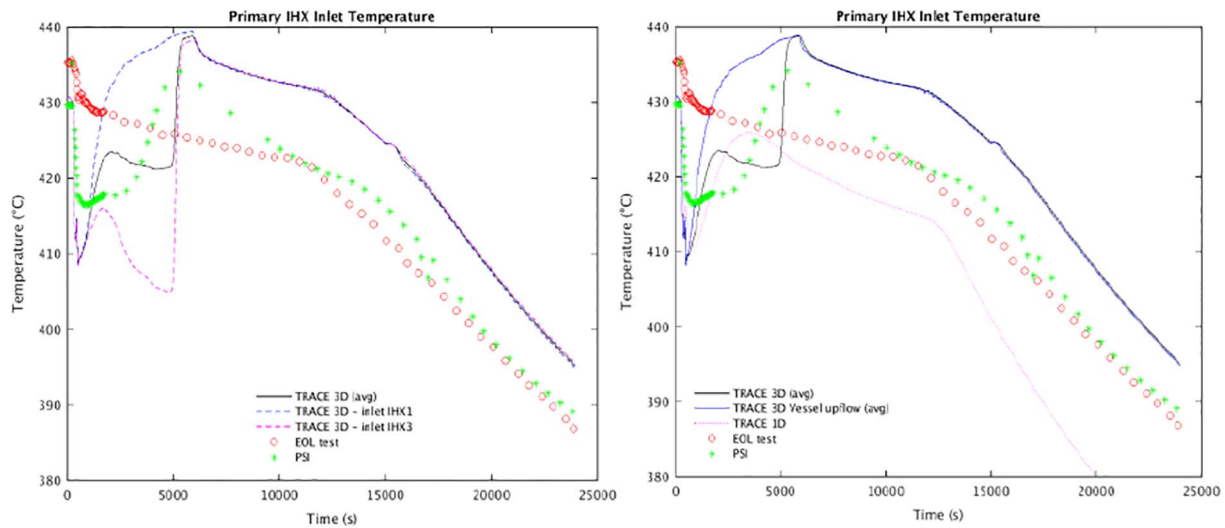


Fig. 13. Evolution of primary IHXs inlet temperature throughout natural circulation transient. Left: TRACE three-dimensional nodal system temperatures at the inlet of each primary IHX model (location 1 marked in Fig. 4); Right: TRACE three-dimensional nodal system temperatures extracted at the vessel node the coolant is conveyed to the primary IHXs model (location 2 marked in Fig. 4). Other institutions' results taken from (International Atomic Energy Agency, 2013).

temperature drop from the measurements at  $\sim 300$  s of the transient, not predicted by any other model. However, this is followed by a temperature rise not seen in the experimental results. This result may be improved if the mixing in the cold pool of fluid coming from the primary IHXs could be better modelled. On average, there is an over prediction till  $\sim 10\,000$  s of the transient, from where the primary pumps inlet temperature are well predicted.

#### Secondary outlet temperature

The evolution throughout the transient of the secondary system outlet temperature is shown in Fig. 15. The cold shock is overestimated by TRACE, as the inlet temperature of the primary IHXs. After the cold shock overpredictions, the results of TRACE's three-dimensional nodal system evolve towards the measurements, correcting the results from the one-dimensional system. Additionally, the temperature trend after the scram is dependent on the primary IHXs inlet temperatures and primary mass flows through the IHXs as the natural circulation builds up, hence the asymmetry in temperatures of the two secondary systems.

#### 4. Conclusions and recommendations

The study described in this paper aimed to assess the capability of a three-dimensional thermal-hydraulics nodal system using an adapted version of TRACE system code when using sodium as coolant, to simulate SFR's normal operation and behavior under transient conditions, namely the natural convection scenario.

Giving as boundary conditions the core power, secondary inlet temperature and mass flow, the developed model was able to simulate Phenix steady state within the accepted margins. When simulating the transient scenario, the developed model was able to predict the transient's main physical phenomena of its 3 phases: rise in temperature in the lower part of the reactor vessel, establishment of natural convection and subsequent cooling of the lower and upper part of the vessel. Additionally, the simulation results were in line with the CRP benchmark results, as shown from Figs. 9–15 (CRP benchmark results represented by PSI and IRSN results). In natural circulation conditions, the developed three-dimensional nodal system core mass flow was 3% of the core mass flow, agreeing with the 2–4% from the CRP benchmark results. However, the core pressure drop has proven harder to compare to other CRP benchmark results as other institutions results come from one-dimensional models and it is unknown which pressure friction factors other codes used and where the pressure should be extracted exactly. Nevertheless, TRACE results show similar qualitatively behavior in core pressure drop throughout the transient (steep reduction of

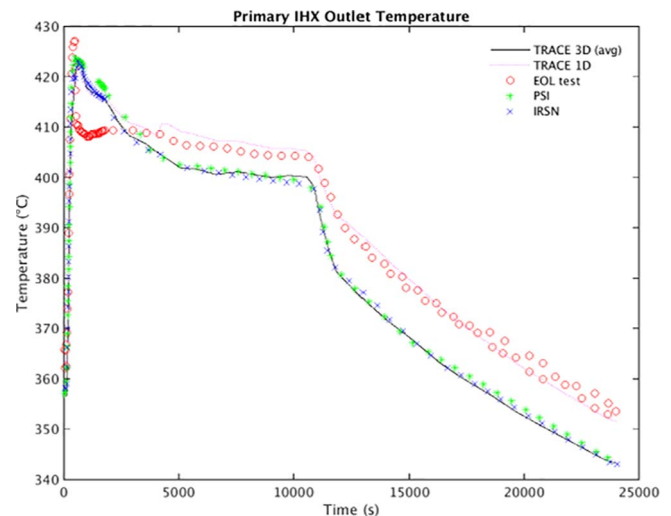


Fig. 14. Primary IHXs outlet temperature (average) throughout the transient. Other institutions' results taken from (International Atomic Energy Agency, 2013).

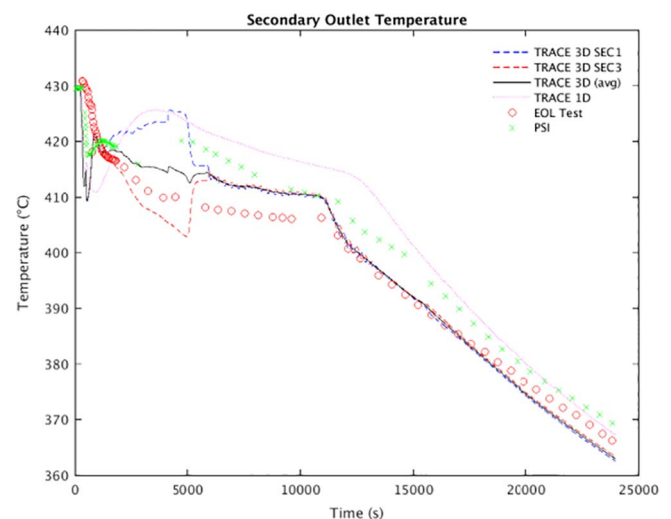


Fig. 15. Evolution of the outlet temperature of the secondary systems. Other institutions' results taken from (International Atomic Energy Agency, 2013).

core pressure drop after the trip of the primary pumps, followed by a stable core pressure drop). The developed model predicts the primary IHX inlet temperature to follow the core outlet temperature as in the CRP benchmark analysis. Nonetheless, experiments show a different behavior of this parameter that can be explained by the fact that the thermocouple in question is located in the upper part of the IHX window (where temperature and mass flows heterogeneities appear) and so is not necessarily representative of the average temperature at the IHX inlet. Also agreeing with the CRP benchmark results, the primary IHX outlet temperature, secondary outlet temperature and pump inlet temperature are strongly connected. Experimentally, the temperatures resulting from the heat exchange are matched by the calculations however it is important to highlight that the location of the extraction of the calculation values is of extreme importance due to the three-dimensional nature of the developed system.

The three-dimensional nodal system is able to clearly illustrate the existing thermal stratification in the hot pool, which is neglected by one-dimensional nodal systems. Due to its inherent geometric capabilities, in the three-dimensional nodal system it is possible to extract values in more realistic and precise locations that, when compared to experimental results, and show a better agreement than what one dimensional models provide. Additionally, the three-dimensional feature enables the modelling of thermal hydraulic asymmetric behavior, as shown by the uneven flow distribution in Phenix's primary IHXs as they are asymmetrically located in the reactor vessel.

Given the calculation results analysis, it is possible to conclude that the developed three-dimensional thermal-hydraulics system is capable to predict and study natural convection phenomena in Sodium Fast Reactors. Nevertheless, it is important to refer that for a very detailed analysis of the recirculation at the top of the core and cross flows within the fuel assemblies generated in a natural circulation scenario, it is necessary the use more refined scale tools for the hot and cold collectors and inter-assembly space (like CFD and sub-channel codes for the assemblies).

Currently, a Phenix core neutronics model using PARCS system code is being developed. This will be coupled to the presented three-dimensional thermal-hydraulics system creating a three-dimensional multi-physics model and allowing the simulation of more complex

transient scenarios, subject of the second part of the article.

## References

- Generation-IV International Forum, 2014. Technology Roadmap Update for Generation IV Nuclear Energy Systems. OECD Nuclear Energy Agency, n.p., ch. 1–2.
- International Atomic Energy Agency, 2006. Fast Reactor Database 2006 Update. International Atomic Energy Agency, Vienna.
- International Atomic Energy Agency, 2012. Status of Fast Reactor Research and Technology Development. International Atomic Energy Agency, Vienna.
- International Atomic Energy Agency, 2013. Benchmark Analyses on the Natural Circulation Test Performed During the PHENIX End-of-life Experiments. International Atomic Energy Agency, Vienna.
- Lefèvre, J.C., Mitchell, C.H., Hubert, G., 1996. European Fast Reactor Design. Nucl. Eng. Des. 162, 133–143.
- Lillington, J.N., 2004. *The Future of Nuclear Power*. Elsevier.
- CEA, 2003–2011. Collaborative Project for a European Sodium Fast Reactor. <http://www.cp-esfr.eu> (accessed 06.03.2017).
- Mikityuk, K., 26–29 June 2017. ESFR-SMART: new Horizon-2020 project. Yekaterinburg (conference proceedings).
- Cahalan, J.E., Ama, T., Palmiotti, G., Taiwo, T.A., Yang, W.S., 2000. Development of a coupled dynamics code with transport theory capability and application to accelerator-driven systems transients. PHYSOR ANS International Topical Meeting on Advances in Reactor Physics and Mathematics and Computation into the Next Millennium. Pittsburgh (conference proceedings).
- Tobita, Y., Kondo, S.A., Yamano, H., Morita, K., Maschek, W., Coste, P., Cadiou, T., 2006. The development of SIMMER-III, an advanced computer program for LMFR safety analysis, and its applications to sodium experiments. Nucl. Technol. 153, 245–255.
- Bohl, W.R., Luck, L.B., 1990. SIMMER-II: A Computer Program for LMFR Disrupted Core Analysis. Los Alamos National Laboratory, Los Alamos.
- Jeong, H.-Y., Ha, K.-S., Choi, C.-W., 2014. Multi-dimensional pool analysis of Phenix end-of-life natural circulation test with MARS-LMR code. Ann. Nucl. Energy 63, 309–316.
- Mochizuki, H., Kikuchi, N., Li, S., 2013. Computation of natural convection test at Phenix reactor using the NETFLOW++ code. Nucl. Eng. Des. 262, 1–11.
- U.S.NRC, 2012. TRACE V5.0 Theory Manual. USNRC, Washington D.C.
- Mikityuk, K., 2009. Heat transfer to liquid metal: review of data and correlations for tube bundles. Nucl. Eng. Des. 239, 680–687.
- Lazaro, A., Ammirabile, L., Bandini, G., Darmet, G., Massara, S., Dufour, Ph., Tosello, A., Gallego, E., Jimenez, G., Mikityuk, K., Schikorr, M., Bubelis, E., Ponomarev, A., Krussmann, R., Stempniewicz, M., 2013. Code assessment and modeling for design basis accident analysis of the European sodium fast reactor design. Part I: system description, modelling and benchmarking. Nucl. Eng. Des. 266, 1–16.
- Bubelis, E., Schikorr, M., 2008. Review and proposal for best fit of wire-wrapped fuel bundle friction factor and pressure drop predictions using various existing correlations. Nucl. Eng. Des. 238, 3299–3320.
- D'Auria, F., Frogheri, M., Gianotti, W., 1999. RELAP/MOD3.2 Post Test Analysis and Accuracy Quantification of SPES TEST SP-SB-03. U.S.NRC, 30.